International Journal of Offshore and Coastal Engineering
Vol.10 | No. 1 | pp. 31 – 37 | May 2026
e-ISSN: 2580-0914

Submitted: Desember 1, 2025 | Revised: January 5, 2026 | Accepted: March 2, 2026

Burst Pressure Assessment of Corroded Steel Pipeline Using DNV-RP-F101 and Finite Element Method with Circumferential Defect Interaction Study

Yoyok Setyo Hadiwidodo[a], Asta Razqi[a], and Herman Pratikno[a*]

[a)] Department of Ocean Engineering, Institut Teknologi Sepuluh Nopember, Surabaya, Indonesia
*email: hermanp@oe.its.ac.id

ABSTRACT

Metal loss corrosion is one of the primary degradation mechanisms in steel pipelines in the oil and gas industry. Wall thickness reduction due to corrosion increases hoop stress and reduces the maximum pressure capacity of the pipeline, potentially leading to bursting failure. This study aims to analyze the bursting pressure of corroded steel pipelines using two approaches: the analytical method based on DNV-RP-F101 and the numerical method using the Finite Element Method (FEM) through ANSYS software. The parameters investigated include the defect depth ratio (d/t) and the circumferential spacing between defects. A three-dimensional numerical model was developed considering elastic-plastic material behavior. The results indicate that an increase in defect depth ratio has a dominant effect in reducing bursting pressure, while closer defect spacing intensifies stress interaction and accelerates local plastification. A comparison between DNV-RP-F101 and FEM shows deviations within acceptable engineering tolerance; however, FEM predicts lower failure pressure as it captures stress concentration and plastic distribution in greater detail.

***Keywords*—Bursting pressure, corrosion, DNV-RP-F101, finite element method, defect interaction, pipeline integrity**

1. INTRODUCTION

Steel pipelines are the primary components in fluid transportation systems within the oil and gas industry, both for onshore and offshore applications. The structural integrity of pipelines is critical, as failure due to internal pressure can result in significant economic losses, environmental damage, and serious safety risks [1]. One of the most common degradation mechanisms during pipeline operation is corrosion, particularly in the form of metal loss defects that cause localized wall thickness reduction [2].

From a structural mechanics perspective, pipelines subjected to internal pressure experience hoop stress, which is directly proportional to the internal pressure and pipe diameter, and inversely proportional to the wall thickness. When wall thickness is reduced due to corrosion, the stress distribution becomes non-uniform, leading to increased local stress around the defect area. This condition significantly reduces the pipeline's capacity to withstand internal pressure and may lead to bursting failure when the operating pressure exceeds the remaining structural capacity [3].

In industrial practice, the assessment of the remaining strength of corroded pipelines is commonly performed using analytical approaches based on standards or recommended practices. One widely used standard is Det Norske Veritas Recommended Practice F101, known as DNV-RP-F101: Corroded Pipelines [4]. This standard provides semi-empirical formulations to estimate the bursting pressure of pipelines with metal loss defects based on defect geometry and material properties. The method is developed from regression of experimental data and is intended to provide conservative estimates for pipeline integrity assessment.

Despite its widespread use, DNV-RP-F101 has several limitations. The formulations are based on simplified assumptions regarding stress distribution and defect interaction, which may not fully capture stress concentration effects, particularly in cases involving complex or closely spaced defects [5]. In practice, corrosion defects rarely occur in isolation; they may appear in clusters with certain spacing, including in the circumferential direction. The interaction of stress fields between closely spaced defects can accelerate local plastification and further reduce the bursting pressure compared to a single defect case [6].

To address the limitations of analytical approaches, numerical methods such as the Finite Element Method (FEM) are widely used in pipeline integrity studies. FEM enables three-dimensional modeling of defect geometry and incorporates nonlinear elastic-plastic material behavior. Through this approach, stress distribution (e.g., Von Mises stress), the development of plastic zones, and failure mechanisms can be analyzed in greater detail [7]. Moreover, FEM can capture stress concentration at defect edges and plastic interaction between defects, which are difficult to represent explicitly in semi-empirical formulations [8].

Previous studies have shown that bursting pressure predictions obtained using numerical methods may differ from analytical methods, particularly at high defect depth ratios (d/t) and in cases where defects interact [9]. Therefore, a comparative evaluation is necessary to assess the level of agreement between the DNV-RP-F101 method and FEM simulations, as well as to identify conditions under which the analytical approach remains adequate or requires support from numerical analysis.

This study focuses on analyzing the bursting pressure of steel pipelines with corrosion defects, considering variations in defect depth ratio (d/t) and circumferential spacing between defects. The analysis is conducted using two approaches: calculations based on DNV-RP-F101 and numerical simulations using ANSYS with an elastic-plastic material model. The parameters evaluated include stress distribution, maximum bursting pressure, and the deviation margin between the two methods.

The main contribution of this study is to provide a more comprehensive understanding of the effect of circumferential defect interaction on bursting capacity and to evaluate the conservatism of the DNV-RP-F101 method compared to nonlinear numerical approaches. The results are expected to serve as a reference for assessing the integrity of corroded pipelines and to support decision-making in inspection planning and repair strategies.

2. RESEARCH METHODOLOGY

2.1 Pipeline Data and Spesification

The object of this study is a carbon steel pipeline with metal loss corrosion defects. The geometric parameters and mechanical properties used in this study refer to the pipeline specifications analyzed in the final project, including outer diameter (D), wall thickness (t), and material properties such as Specified Minimum Yield Strength (SMYS) and Specified Minimum Tensile Strength (SMTS). These parameters are the primary variables in evaluating the bursting pressure capacity of corroded pipelines [1].

The pipeline material is modeled as an isotropic elastic–plastic material with Young's modulus (E) and Poisson's ratio (v). The flow stress is calculated as the average of SMYS and SMTS, following the approach in Det Norske Veritas Recommended Practice DNV-RP-F101 [2]. These material parameters are consistently applied in both analytical calculations and numerical simulations to ensure the validity of the comparison results.

Table 1.Pipeline Geometry Specifications and Material Properties

Parameters	*Value*	*Units*	*Value*	*Units*
Outside Diameter	*323.85*	*mm*	12.75	*inch*
Wall Thickness	*12.7*	*mm*	0.5	*inch*
Type of Pipe Material	*Carbon Steel Pipe*	-	-	-
Service	*Natural Gas*	-	-	-
SMYS	*450*	*MPa*	52.2	-
SMTS	*535*	*MPa*	66.7	*ksi*
Young Modulus	2.07×10^5	*MPa*	30022.9	*ksi*
Poisson Ratio	*0.3*	-	-	*ksi*
Density	*7850*	kg/m^3	-	-

2.2 Corrosion Defect Geometry Variations

The defects analyzed are metal loss types, idealized as localized geometric features on the pipe surface. The variation of defect parameters considered includes:

1. Defect depth ratio to pipe thickness (d/t)
2. Circumferential spacing between defects

The defect depth ratio (d/t) is selected as the primary parameter due to its significant influence on the remaining strength of the pipeline, as it directly reduces the effective cross-sectional area [3]. In addition, two defects are modeled in the circumferential direction with specific spacing to evaluate the stress interaction between defects. This interaction may accelerate local plastification when the spacing falls within overlapping stress influence zones [4].

This variation approach aims to represent realistic corrosion conditions, where defects do not always occur as isolated single defects.

Table 2. Variation of Defect Depth Ratio and Circumferential Spacing

Variation	*Circumferential spacing, θ (°)*	*Length Defect, L (mm)*	*Width Defect, W (mm)*	*Depth Defect, d (mm)*
1	180	200	110	8.3
2	180	200	110	6.3
3	180	200	110	4
4	180	100	110	8.3
5	180	100	110	6.3
6	180	100	110	4

2.3 Bursting Pressure Calculation Using DNV-RP-F101

The calculation of bursting pressure in this study refers to Det Norske Veritas DNV-RP-F101 (2017) as a guideline for evaluating the remaining strength of pipelines affected by metal loss corrosion [2]. Bursting pressure is defined as the maximum internal pressure that a pipeline can withstand before failure due to wall thickness reduction caused by corrosion.

1. Single Defect

For a single defect, the bursting pressure is calculated using:

$$P_f = \frac{P_m 2 t f_u}{(D-t)}\left(\frac{1-d/t}{1-d/(tQ)}\right) \tag{1}$$

with the length correction factor:

$$Q = \sqrt{1+0.31\left(\frac{l}{\sqrt{Dt}}\right)^2} \tag{2}$$

where P_f is the failure pressure, t is the pipe thickness, f_u is the tensile strength, D is the outer diameter, d is the defect depth, and l is the defect length.

In this study, the defects are located on the external surface of the pipe and positioned opposite each other radially; therefore, they can initially be evaluated using the single defect approach based on DNV-RP-F101 [2].

2. Defect Interaction Evaluation

For multiple defects, circumferential interaction is assessed by comparing the angular spacing between defects (ϕ) with the interaction limit angle (Z):

$$Z = 360\sqrt{\frac{t}{D}} \tag{1}$$

If $\phi < Z$, the defects are considered interacting and are analyzed as a combined defect [2].

The equivalent length of the combined defect is calculated as:

$$l_{nm} = l_m + \sum_{i=n}^{m-1}(l_i + s_i)$$

and the equivalent depth is given by:

$$d_{nm} = \frac{\sum_{i=n}^{m} d_i l_i}{l_{nm}}$$

The bursting pressure for the combined defect is calculated as:

$$P_{nm} = \frac{2 t f_u}{(D-t)}\left(\frac{1-\frac{d_{nm}}{t}}{1-\frac{d_{mn}}{t Q_{nm}}}\right)$$

with the length correction factor:

$$Q_{nm} = \sqrt{1+0.31\left(\frac{l_{nm}}{\sqrt{Dt}}\right)^2}$$

The lowest failure pressure among all interacting defect combinations is used as the basis for evaluating the safe pressure limit of the pipeline [2].

2.4 Numerical Modeling Using the Finite Element Method

Numerical simulation using the Finite Element Method (FEM) was conducted to evaluate the mechanical behavior of pipelines with external corrosion defects under internal pressure loading. This section systematically describes the FEM modeling and analysis procedures, including geometry creation, material property definition, application of boundary conditions, internal pressure loading, as well as discretization and simulation result evaluation.

The FEM simulation aims to obtain the von Mises stress distribution in the pipeline, identify locations of maximum stress concentration around corrosion defects, and determine the internal pressure that leads to structural failure (bursting pressure). The bursting pressure is defined based on a specified failure criterion, allowing the simulation results to be used for pipeline integrity assessment and as a comparison to analytical calculations based on the DNV-RP-F101 standard.

All FEM simulation procedures in this study were applied consistently across all variations of defect dimensions and circumferential spacing, enabling an objective and quantitative analysis of the influence of each parameter on von Mises stress and bursting pressure.

2.5 Plastic Strain–True Stress Relationship

The stress–strain curve of API 5L X65 steel used in this study is based on the work of Chang-Kyun Oh et al. in the paper *"Development of Stress-Modified Fracture Strain for Ductile Failure of API X65 Steel,"* which presents the true stress–true strain relationship obtained from tensile testing as the basis for material behavior characterization.

For finite element analysis in ANSYS, this curve is converted into a relationship between true stress and plastic strain. The conversion is performed by separating the elastic strain from the total strain using linear elastic theory, so that the plastic strain is obtained as the difference between the two. Thus, only the plastic deformation component is used in the nonlinear material modeling.

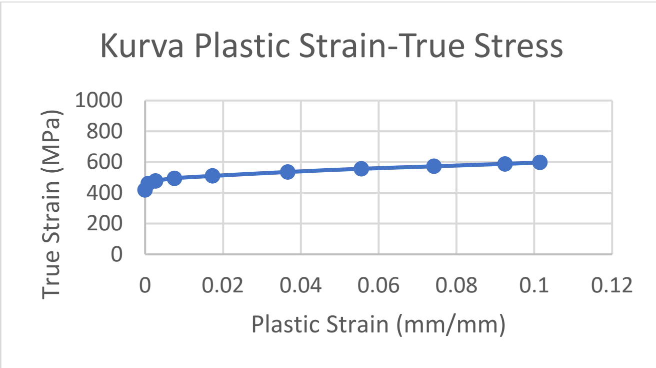

Gambar 1. Plastic Strain–True Stress Material Baja API 5L X65 Curve

The converted data are presented in the form of a plastic strain–true stress table, which is used as input for the elastic–plastic material model in ANSYS. The data are then visualized as a graph to ensure consistency with the reference curve trend.

Overall, three data representations are used: the true stress–true strain curve from the literature, the converted data table, and the plastic strain–stress graph, which serves as the material behavior representation in the finite element analysis.

3. RESULTS AND DISCUSSION

3.1 Equation Burst Pressure Using DNV RP-F101

To complement the analysis, bursting pressure calculations were also performed for other variations of dent dimensions and circumferential locations using the same calculation procedure. The complete results of these calculations are presented in the following table..

Tabel 3. Burst Pressure Calculation Based on DNV-RP-F101

Variasi	*Jarak Circumferential , θ (°)*	*Panjang Defect, L (mm)*	*Lebar Defect , W (mm)*	*Kedalaman Defect, d (mm)*	*Bursting Pressure , Pf (MPa)*
1	180	200	110	8.3	22.454
2	180	200	110	6.3	29.250
3	180	200	110	4	35.497
4	180	100	110	8.3	29.873
5	180	100	110	6.3	35.190
6	180	100	110	4	38.075

These calculation results are used as an initial reference for numerical analysis using the Finite Element Method (FEM). The bursting pressure values obtained from the DNV approach are used to validate the FEM simulation results, ensuring they remain within an error margin of ±5%.

The bursting pressure calculated using the DNV-RP-F101 method for all defect variations shows a decrease in pressure capacity with increasing defect depth, length, and interaction between defects. These values serve as a baseline for evaluating the validity of the numerical simulation results.

Subsequently, pipeline modeling with defect variations is carried out using ANSYS through the FEM approach. The process includes geometry creation, material property definition, meshing, and the application of boundary conditions and internal pressure loading. The solving stage is performed to obtain the stress distribution in the pipeline, which is then evaluated using the von Mises equivalent stress criterion to determine failure conditions.

All modeling results and stress distributions are visualized in contour plots for each defect variation to support further analysis of the pipeline's structural behavior.

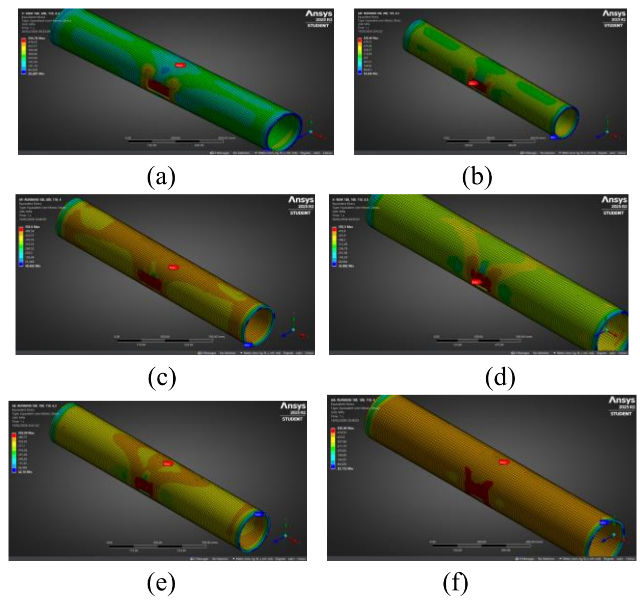

Gambar *1*. Hasil pengujian *FEM* (a) Hasil Running Model Pipa dengan Dua Defect Korosi Eksternal (θ = 180°, L = 200 mm, D = 8.3 mm) (*b*) Dua Defect Korosi Eksternal (θ = 180°, L = 200 mm, D = 6.3 mm), (*c*) Dua Defect Korosi Eksternal (θ = 180°, L = 200 mm, D = 4 mm)

Tabel *4*.
Perhitungan Burst Pressure Berdasarkan *Analisis FEM*

Variasi	*Jarak Circumferential , θ (°)*	*Panjang Defect, L (mm)*	*Lebar Defect , W (mm)*	*Kedalaman Defect, d (mm)*	*Bursting Pressure , Pf (MPa)*
1	180	200	110	8.3	22.3
2	180	200	110	6.3	28
3	180	200	110	4	35.6
4	180	100	110	8.3	30.5
5	180	100	110	6.3	34.7
6	180	100	110	4	38.075

The recapitulated results indicate that the failure pressure obtained from FEM simulations is influenced by defect dimensions, particularly length, depth, and circumferential spacing between defects. Increasing defect length and depth reduces the failure pressure due to higher stress concentration, while smaller circumferential spacing accelerates this reduction as a result of stress field interaction between defects.

Tabel *5*. Comparison of Percentage Error Margin Between the DNV Method and the Finite Element Method (FEM)

Variasi	*Jarak Circumferential, θ (°)*	*Panjang Defect, L (mm)*	*Lebar Defect, W (mm)*	*Kedalaman Defect, d (mm)*	*Bursting Pressure, Pf (MPa)*	*Presentase Margin Error,(%)*
1	180	200	110	8.3	22.3	0.685
2	180	200	110	6.3	28	4.273
3	180	200	110	4	35.6	0.290
4	180	100	110	8.3	30.5	2.098
5	180	100	110	6.3	34.7	1.392
6	180	100	110	4	38.075	3.003

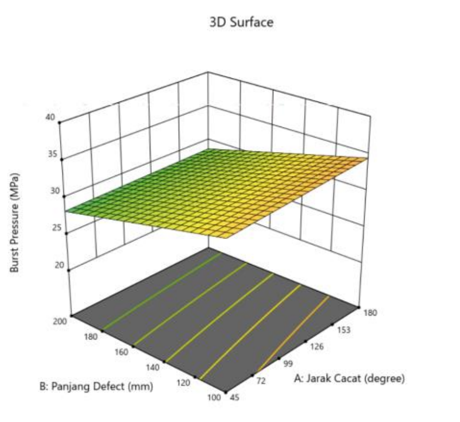

Gambar *2. Pengaruh Variasi Kedalaman dan Panjang antar Cacat terhadap Burst Pressure*

Figure 2 illustrates the combined effect of defect depth and defect length on bursting pressure. It can be observed that increasing defect depth results in a more significant reduction in bursting pressure compared to variations in defect length. This indicates that defect depth is the dominant parameter in determining the remaining strength of the pipeline.

Meanwhile, increasing defect length also leads to a decrease in bursting pressure, but with a more gradual trend. The interaction between these two parameters shows that the combination of maximum defect depth and length produces the most critical condition for pipeline failure.

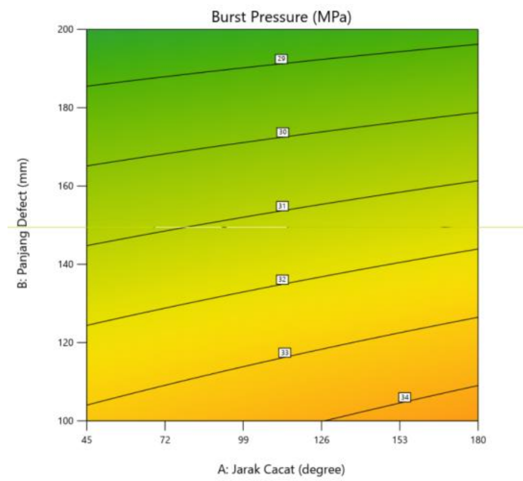

Gambar *3. Pengaruh Variasi Kedalaman dan Jarak antar Cacat terhadap Burst Pressure*

Figure 3 illustrates the relationship between defect depth and circumferential spacing on bursting pressure. The results show that defect depth remains the dominant factor in reducing failure pressure. However, the spacing between defects also has a significant effect, particularly at smaller spacing configurations (45°), where stress field interaction occurs between defects.

This condition leads to a more complex stress distribution and increased stress concentration, resulting in lower bursting pressure compared to configurations with larger spacing (180°).

Figure 4 shows the effect of variations in defect length and circumferential spacing on bursting pressure. It can be observed that increasing defect length consistently reduces the failure pressure due to the greater material loss area. In addition, the spacing between defects influences the structural response of the pipeline, where smaller spacing leads to stronger stress interaction and a reduction in bursting pressure. However, compared to defect depth, the influence of defect length and spacing is relatively more moderate.

4. Results Validation

External validation is performed by comparing the trends of the results obtained in this study with those reported by Zheng Feng Chen. In that study, defects were modeled in an overlapping configuration (*asymmetrical overlapping defects*), whereas this study considers defects arranged in an opposing configuration with a different pipe diameter.

Tabel 2. External Validation Against the Study by Zheng Feng Chen

Parameter	Zheng Feng Chen (Overlapping)	DNV (Penelitian Ini)	FEM (Penelitian Ini)	Konsistensi Tren	Parameter
Kedalaman ↑	P_burst ↓ signifikan	P_burst ↓ signifikan	P_burst ↓ signifikan	Konsisten	P_burst ↓ signifikan
Panjang ↑	P_burst ↓	P_burst ↓	P_burst ↓	Konsisten	P_burst ↓
Interaksi Cacat	Sangat signifikan	Terbatas	Signifikan	Parsial	Sangat signifikan
Kedalaman ↑	P_burst ↓ signifikan	P_burst ↓ signifikan	P_burst ↓ signifikan	Konsisten	P_burst ↓ signifikan

Based on Table 5, this study shows a consistent trend with the results reported by Chen, particularly in terms of the decrease in bursting pressure with increasing defect depth and length. The main difference lies in the intensity of defect interaction, where the overlapping configuration in Chen's study produces more complex interaction effects compared to the opposing configuration used in this study.

Although no direct numerical comparison is performed, the agreement in mechanical trends indicates that the developed model has conceptual validity and is capable of realistically representing the structural behavior of the pipeline.

5. CONCLUSION

Based on the results of this study, several conclusions can be drawn:

1. Bursting pressure was successfully determined using DNV-RP-F101 and FEM for all defect variations. The pressure decreases with increasing defect length and depth, with FEM yielding more conservative results due to its ability to capture three-dimensional stress concentrations.
2. Variations in defect geometry affect bursting pressure with different levels of sensitivity. Defect depth is the most dominant parameter, followed by defect length, while circumferential spacing is not significant in DNV but has a noticeable effect in FEM due to stress interaction between defects.
3. The comparison between DNV and FEM shows consistent trends with relatively small deviations (±0.29%–4.97%). DNV is suitable for practical evaluations, whereas FEM provides higher accuracy for detailed analysis of pipeline integrity with multiple defects.

ACKNOWLEDGEMENTS

The author would like to express sincere gratitude to all parties who have provided support and assistance in the completion of this research.

REFERENCES

[1] M. Al-Owaisi *et al.*, "Stress-strain behavior of corroded pipelines under internal pressure," *Journal of Pipeline Engineering*, 2018.
[2] ASME, *ASME B31G: Manual for Determining the Remaining Strength of Corroded Pipelines*, American Society of Mechanical Engineers, 2018.
[3] Y. Bai and Q. Bai, *Subsea Pipeline Design, Analysis, and Installation*, Gulf Professional Publishing, 2014.
[4] W. D. Callister and D. G. Rethwisch, *Materials Science and Engineering: An Introduction*, 9th ed., Wiley, 2018.
[5] Y. Chen, G. Zhang, and Y. Qiu, "Mechanical model assessment of pipelines with complex corrosion defects," *Engineering Failure Analysis*, 2024.
[6] Z.-F. Chen *et al.*, "Study on burst pressure of subsea pipelines with asymmetrical corrosion defects," *Ocean Engineering*, vol. 295, 117456, 2024.
[7] M. S. G. Chiodo, C. Ruggieri, and T. A. Netto, "Failure assessment of corroded pipelines subjected to internal pressure," *Engineering Failure Analysis*, vol. 19, pp. 37–52, 2012.
[8] A. Cosham and P. Hopkins, "The effect of defects on pipeline integrity," *International Journal of Pressure Vessels and Piping*, 2003.
[9] DNV, *Recommended Practice DNV-RP-F101: Corroded Pipelines*, Det Norske Veritas, 2010.
[10] DNV, *DNV-RP-F101: Corroded Pipelines (Update)*, 2017.
[11] A. Driyastomo, *Analisis Tekanan Von Mises pada Pipa Baja*, Tugas Akhir, 2020.
[12] H. Fang, Y. Cheng, and Z. Liu, "Burst capacity of pipelines with interacting corrosion defects," *International Journal of Pressure Vessels and Piping*, vol. 145, pp. 1–10, 2016.
[13] J. R. Fekete, L. Varga, and L. Dinya, "Effect of corrosion defect width on the burst pressure of pipelines," *Engineering Failure Analysis*, vol. 55, pp. 177–187, 2015.
[14] International Energy Agency, *World Energy Outlook 2008*, 2008.
[15] S. Kim *et al.*, "Corrosion behavior of subsea pipelines," *Corrosion Science*, 2012.
[16] S. Kingklang and V. Uthaisangsuk, "Plastic deformation and fracture behavior of X65 pipeline steel: Experiments and modeling," *Engineering Fracture Mechanics*, vol. 131, pp. 594–606, 2014.
[17] L. Z. Kong *et al.*, "True stress–strain curves test and material property analysis of API X65 and API X90 gas pipeline steels," *Journal of Materials Engineering and Performance*, vol. 28, pp. 2047–2058, 2019.
[18] A. Laksono, *Korosi pada Pipa Industri*, Penerbit Teknik, 2018.
[19] Y. Liu, F. Khan, and P. Thodi, "Failure assessment of corroded pipelines: A review," *Journal of Loss Prevention in the Process Industries*, vol. 49, pp. 662–674, 2017.
[20] R. E. Melchers and R. Jeffrey, "Marine corrosion of steel pipelines – impacts of oxygen concentration," *Corrosion Science*, vol. 50, no. 7, pp. 2003–2012, 2008.
[21] T. A. Netto, U. S. Ferraz, and S. F. Estefen, "The effect of corrosion defects on the burst pressure of pipelines," *International Journal of Pressure Vessels and Piping*, 2005.
[22] C.-K. Oh *et al.*, "Development of stress-modified fracture strain for ductile failure of API X65 steel," *Engineering Fracture Mechanics*, vol. 179, pp. 22–37, 2017.

[23] A. C. Palmer and R. A. King, *Subsea Pipeline Engineering*, PennWell Books, 2008.

[24] V. Ramakrishna and R. Vijayaframan, "Burst pressure evaluation of corroded pipelines," *Engineering Failure Analysis*, vol. 3, no. 1, pp. 45–55, 1996.

[25] R. C. C. Silva, J. N. C. Guerreiro, and A. F. D. Loula, "A study of pipe interacting corrosion defects using the FEM and neural networks," *International Journal of Pressure Vessels and Piping*, vol. 81, no. 2, pp. 141–151, 2004.

[26] M. Y. Sormin, *Analisis Kekuatan Pipa Bawah Laut yang Mengalami Korosi Eksternal dengan Metode Elemen Hingga*, Tugas Akhir, ITS, 2021.

[27] A. C. Ugural and S. K. Fenster, *Advanced Strength and Applied Elasticity*, 4th ed., Prentice Hall, 2003.

[28] M. Xie, M. H. Mohd, and X. Shen, "Numerical studies of corroded pipelines under internal pressure," *Journal of Pressure Vessel Technology*, vol. 136, no. 4, 041401, 2014.

[29] G. Zhang, Y. Qiu, and Y. Chen, "Risk assessment of subsea pipeline failure due to corrosion," *Ocean Engineering*, vol. 108, pp. 1–12, 2015.

[30] Y. Zhang *et al.*, "A novel assessment method to identifying the interaction between adjacent corrosion defects and its effect on the burst capacity of pipelines," *Journal of Loss Prevention in the Process Industries*, vol. 69, 104341, 2021.

[31] Y. Zhang, Z. Chen, and X. Li, "Finite element analysis of pipelines with interacting corrosion defects," *International Journal of Pressure Vessels and Piping*, vol. 123–124, pp. 38–48, 2014.

[32] Y. Zhang, W. Wang, and J. Shuai, "Interaction effects of complex corrosion defects on burst pressure of subsea pipelines," *Ocean Engineering*, vol. 286, 115324, 2024.